



## รายงานวิจัยฉบับสมบูรณ์

โครงการ แบบจำลองปฏิกิริยาการแพร่สำหรับการกระจายตัว  
เชิงกลของประชากรแบคทีเรีย<sup>1</sup>  
(Reaction-diffusion model for mechanically spreading of  
bacterial populations)

โดย ผู้ช่วยศาสตราจารย์ ดร. ไวพจน์ งามสอด

พฤษภาคม 2559

สัญญาเลขที่ TRG5780037

รายงานวิจัยฉบับสมบูรณ์

โครงการ แบบจำลองปฏิกิริยาการแพร่สำหรับการกระจายตัว  
เชิงกลของประชากรแบคทีเรีย (Reaction-diffusion model  
for mechanically spreading of bacterial populations)

ผู้ช่วยศาสตราจารย์ ดร. ไวยพจน์ งามสอาด  
สาขาวิชาฟิสิกส์ คณะวิทยาศาสตร์ มหาวิทยาลัยพะเยา

สนับสนุนโดยสำนักงานกองทุนสนับสนุนการวิจัยและ  
มหาวิทยาลัยพะเยา

(ความเห็นในรายงานนี้เป็นของผู้วิจัย  
สก. และต้นสังกัด ไม่จำเป็นต้องเห็นด้วยเสมอไป)

## Abstract

---

**Project Code:** TRG5780037

**Project Title:** Reaction-diffusion model for mechanically spreading of bacterial populations

**Investigator:** Assistant Professor Dr. Waipot Ngamsaad, Division of Physics, School of Science, University of Phayao

**E-mail Address:** waipot.ng@up.ac.th

**Project Period:** 2 years

The growth and spreading of bacterial population are significant problems in biological science. Reaction-diffusion model, formulated by the nonlinear partial differential equation, has been a theoretical tool for investigating the structure and pattern formation in bacterial colony. However, the conventional models assume that the individual of population behaves like an ideal particle, which has no shape. Unfortunately, this assumption is correct only in the system of low population density. In real situations, the individual of bacterial population has heterogeneous shape and grows under dense environmental conditions. Accordingly, the mechanical interaction between cells has crucial roles on the spreading of bacterial colony. Therefore, in this research, we extend the reaction-diffusion model by incorporating the mechanical effect from the cell shape for investigating the problem of spreading bacterial populations.

**Keywords:** Reaction-diffusion model, Nonlinear partial differential equation, Population dynamics

## บทคัดย่อ

รหัสโครงการ: TRG5780037

ชื่อโครงการ: แบบจำลองปฏิกริยาการแพร่สำหรับการกระจายตัวเชิงกลของประชากรแบบที่เรียกชื่อนักวิจัย: ผู้ช่วยศาสตราจารย์ ดร. ไวยจน์ งามสอดاد สาขาวิชาพิสิกส์ คณะวิทยาศาสตร์ มหาวิทยาลัยพะเยา

E-mail Address: waipot.ng@up.ac.th

ระยะเวลาโครงการ: 2 ปี

การเติบโตและแพร่กระจายของประชากรแบบที่เรียกเป็นปัญหาสำคัญในวิทยาศาสตร์ชีวภาพ แบบจำลองปฏิกริยาการแพร่ เขียนอยู่ในรูปของสมการเชิงอนุพันธ์ย่อยไม่เป็นเชิงเส้น ได้เป็นเครื่องมือเชิงทฤษฎีสำหรับการศึกษาโครงสร้างและการก่อรูปแบบในโคลนีของแบบที่เรียกแต่อ่อนกว่า ประกอบด้วย แบบจำลองแบบปกติสมมุติให้ประชากรแต่ละตัวมีพฤติกรรมคล้ายอนุภาคในอุดมคติที่ไม่มีรูปร่าง แต่ข้อสมมุตินี้ถูกต้องเฉพาะในระบบที่ประชากรมีความหนาแน่นต่ำ ในความเป็นจริงประชากรแบบที่เรียกมีรูปร่างที่แตกต่างกันและเจริญเติบโตในสภาวะแวดล้อมที่หนาแน่น ด้วยเหตุนี้แรงกระทำเชิงกลระหว่างเซลล์จึงมีบทบาทสำคัญยิ่งในการแพร่กระจายของประชากรแบบที่เรียก ดังนั้นในงานวิจัยนี้เราจะขยายแบบจำลองปฏิกริยาการแพร่โดยการเพิ่มผลกระทบเชิงกลจากรูปร่างเซลล์สำหรับการศึกษาปัญหาการแพร่กระจายของประชากรแบบที่เรียก

คำหลัก: แบบจำลองปฏิกริยาการแพร่, สมการเชิงอนุพันธ์ย่อยไม่เป็นเชิงเส้น, พลศาสตร์ประชากร

## Executive Summary

---

### 1. ความสำคัญและที่มาของปัญหา

แบบที่เรียเป็นจุลซึพที่เป็นสาเหตุของโรคในมนุษย์ พืช และ สัตว์ แต่อย่างไรก็ตามในอุตสาหกรรมแบบที่เรียสามารถสร้างผลิตภัณฑ์ที่เป็นประโยชน์ต่อมนุษย์ เช่น ยาปฏิชีวนะ และการหมักอาหาร เป็นต้น ดังนั้นการเข้าใจถึงผลศาสตร์ของประชากรแบบที่เรียจึงมีความสำคัญต่อเทคโนโลยีชีวภาพและการแพทย์เป็นอย่างยิ่ง จำนวนเซลล์ของแบบที่เรียมักเปลี่ยนแปลงตามกระบวนการเกิด การตาย และ การเคลื่อนที่ ขึ้นอยู่กับสภาพสิ่งแวดล้อม การทำนายการเปลี่ยนแปลงของประชากรแบบที่เรียในบริเวณและเวลาที่ระบุเป็นปัญหาที่ท้าทายยิ่งอันหนึ่งในวิทยาศาสตร์ชีวภาพ แบบจำลองทางคณิตศาสตร์เป็นวิธีการที่มีประสิทธิภาพในการศึกษาวิวัฒนาการของประชากรแบบที่เรียเชิงปริมาณ ซึ่งเป็นแรงจูงใจให้เราทำการศึกษาพลศาสตร์ของประชากรแบบที่เรียเชิงทฤษฎีโดยใช้วิธีการทำจำลองแบบเชิงคณิตศาสตร์

ในทางทฤษฎี กระบวนการเกิด การตาย และ การเคลื่อนที่ของประชากรสิ่งมีชีวิตสามารถจำลองแบบได้โดยสมการปฏิกิริยาการแพร่ในระดับภาพรวม การแพร่แสดงถึงการเคลื่อนที่ของเซลล์แบบที่เรีย และปฏิกิริยาแสดงถึงตัวรวมของการเปลี่ยนแปลงประชากรอันเนื่องมาจากการเกิดและการตาย ผลเฉลยของสมการนี้ได้ให้ความเข้าใจอันลึกซึ้งในโครงสร้างและรูปแบบของพลศาสตร์ของประชากร โดยเฉพาะอย่างยิ่งมันสามารถที่จะทำนายอัตราเร็วของการแพร่กระจายของโควิด-19 ได้ด้วย

แบบจำลองสำหรับพลศาสตร์ของประชากรแบบที่เรียส่วนใหญ่พิจารณาเพียงการแพร่ อุดมคติ ในแนวคิดนี้ได้สมมุติให้แบบที่เรียแต่ละตัวเป็นอนุภาคจุดที่ไม่มีรูปร่าง แต่โดยทั่วไปแล้วแบบที่เรียมีรูปร่างเป็นทรงแท่ง ดังนั้นอันตรกิริยาเชิงกลระหว่างเซลล์แบบที่เรียได้ถูกละเอียดในแบบจำลองปฏิกิริยาการแพร่แบบเก่า นอกจากนี้ข้อมูลจากการทดลองได้แสดงให้เห็นว่าการขยายตัวของโควิด-19 แบบที่เรียที่ถูกกักในบริเวณจำกัดเป็นผลมาจากการผลักกันของเซลล์มากกว่าการที่มาจากการเคลื่อนที่ของเซลล์ ดังนั้นแบบจำลองที่ลังบันตรกิริยาระหว่างเซลล์อาจไม่สามารถอธิบายการแพร่กระจายของประชากรแบบที่เรียได้อย่างถูกต้อง

ในงานวิจัยนี้ เราจะขยายแบบจำลองปฏิกิริยาการแพร่สำหรับพลศาสตร์ของประชากรแบบที่เรียแบบเก่าโดยรวมอันตรกิริยาระหว่างเซลล์เข้าไปด้วย โดยเราจะสนใจในกรณีอย่างง่ายคือ พลศาสตร์ของระบบสามารถอธิบายด้วยสมการเชิงอนุพันธ์ย่อยแบบไม่เชิงเส้นใน 1 มิติ ซึ่งมีความสอดคล้องกับการวิเคราะห์ ผลเฉลยจากสมการนี้จะนำมาสู่ความเข้าใจที่ดีขึ้นถึงการที่อันตรกิริยาระหว่างเซลล์ควบคุมการแพร่กระจายของความหนาแน่นของแบบที่เรียตามตำแหน่งและเวลา และอัตราเร็วของการขยายตัวของโควิด-19 แบบที่เรียได้อย่างไร

## 2. วัตถุประสงค์

- 2.1 เพื่อขยายสมการปฏิกริยาการแพร่สำหรับพลศาสตร์ของประชากรแบบที่เรียโดยมีการรวมอันตรกิริยาเชิงกลระหว่างเซลล์เข้าไปด้วย
- 2.2 เพื่อประยุกต์ใช้ผลจากแบบจำลองที่ได้เสนอขึ้นใหม่นี้ศึกษาการแพร่กระจายของความหนาแน่นของแบบที่เรียตามตำแหน่งและเวลา และ อัตราเร็วของการขยายตัวของโคลนน์แบบที่เรีย

## 3. ระเบียบวิธีวิจัย

- 3.1 ศึกษาแบบจำลองปฏิกริยาการแพร่สำหรับพลศาสตร์ของประชากรแบบที่เรียโดยมีการรวมอันตรกิริยาเชิงกลระหว่างเซลล์เข้าไปด้วย
- 3.2 หาข้อมูลการทดลองที่เกี่ยวข้องกับการก่อรูปแบบในโคลนน์แบบที่เรียที่ตระหนักถึงผลกระทบจากรูปร่างเซลล์ของแบบที่เรียจากการวิจัยที่พิมพ์แล้ว เพื่อนำมาสนับสนุนสมมุติฐานที่ตั้งไว้
- 3.3 วิเคราะห์แบบจำลองโดยใช้เทคนิคทางคณิตศาสตร์ โดยการหาผลเฉลยเชิงวิเคราะห์ของสมการเชิงอนุพันธ์ย่อยแบบไม่เชิงเส้นที่เสนอขึ้นมาสำหรับในการนี้ที่ความหนาแน่นของแบบที่เรียมีค่าต่ำ
- 3.4 เชื่อมโปรแกรมเพื่อหาผลเฉลยเชิงตัวเลขของแบบจำลองโดยใช้ระเบียบวิธีไฟน์ต์ดิฟเฟอร์เรนซ์ในกรณีที่ความหนาแน่นของแบบที่เรียมีค่าสูง
- 3.5 วัดปริมาณทางกายภาพจากผลเฉลยเชิงตัวเลข เช่น การเปลี่ยนแปลงความหนาแน่นของแบบที่เรีย และอัตราเร็วของการขยายตัวของประชากรแบบที่เรีย
- 3.6 เทียบเปรียบข้อมูลจากการทดลองกับผลเฉลยที่ได้จากแบบจำลอง
- 3.7 เชื่อมบทความวิจัยเพื่อส่งติพิมพ์

## 1. Introduction

Bacteria are microorganisms that cause the diseases in human, plant and animal. However, in industry, some bacteria can make useful products to human, such as fermented food and chemical used in pharmacy and agriculture. Therefore, understanding the dynamics of bacterial population is important to biotechnology and medicine.

The numbers of bacterial cells are always changed by the process of birth, death and cell migration, depending on the environmental conditions. To predict the change in bacterial population at the specific region and time is one of the most challenge problem in biological science. The mathematical modeling is an efficient method for studying the evolution of bacterial population quantitatively. This motivates us to investigate the dynamics of bacterial population theoretically by using the mathematical modeling approach.

In theory, the process of birth, death and migration of the biological population can be modeled by the reaction-diffusion equation at continuum level. The diffusion represents the migration of the bacterial cell; and the reaction represents the net change in population by growth and death. The solution to this equation has been provided insight into the structure and pattern formation in population dynamics. Especially, it can predict the expansion speed of the bacterial colony. Most models for bacterial population dynamics deal with the ideal diffusion of population. In this approach, the individual member of bacteria is assumed to be a point-like particle that has no shape. Typically, the shape of bacteria is rod-like. Thus, the mechanical interaction between bacterial cells has been omitted from the conventional reaction-diffusion model. In addition, the recent experimental observations show that the expansion of the bacterial colony, confined in the limited space, is caused by cell pushing rather than by cell migration. Hence, the model without cell interaction may not be the accurate description for spreading of bacterial population.

In this research, we extend the conventional reaction-diffusion model for bacterial population dynamics by incorporating the mechanical interaction between cells--which is omitted from past models. We focus on the simplified case where the dynamics of system can be described by a one-dimensional nonlinear partial differential equation; which is convenient for analysis. The solutions to this equation could provide

the better understanding of how the mechanical interactions control the spreading of bacterial density in space and time and expansion speed of the bacterial colony.

## 2. Literature review

The recent experiments reveal that the bacteria adapt to unfavorable environments by cooperatively expanding their colony with the well-defined structures (Ben-Jacob *et al.*, 2000; Murray, 2002). Some species of bacteria such as *Escherichia coli* and *Bacillus subtilis*, grown on Petri dish, exhibit the fascinated patterns, including circular disk, concentric rings and fractal-like objects (Kawasaki *et al.*, 1997; Ben-Jacob *et al.*, 2000; Murray, 2002). It has been suggested that the pattern formations, generated by bacterial colony, reflect the social intelligence and communication of this microorganism (Ben-Jacob *et al.*, 2012). It has hypothesized that, somehow, the bacteria use the cooperation to resist the environmental stresses (Ben-Jacob *et al.*, 2012). Understanding of the underlying mechanism of bacterial pattern formation is basic knowledge to biotechnology and medicine.

To study this problem in quantitative way, the reaction-diffusion models have been proposed for the theoretical description of bacterial pattern formation at continuum level (Kawasaki *et al.*, 1997; Golding *et al.*, 1998; Ben-Jacob *et al.*, 2000; Murray, 2002). Although there are several set of coupled reaction-diffusion equations have presented to study this problem, Kawasaki *et al.* have suggested the simplified case (Kawasaki *et al.*, 1997). The bacterial colony evolves in two dimensions; however if we neglect the occasional branching, dynamics of the system evolves in one dimension equivalently. They have found that this dynamics can be described by a single nonlinear reaction-diffusion equation (Kawasaki *et al.*, 1997). This simple model admits the mathematical analysis that provides the details of structures and pattern formation in bacterial colony analytically (Kawasaki *et al.*, 1997; Ben-Jacob *et al.*, 2000; Murray, 2002).

The dynamics of bacterial population can be described as follows (Ben-Jacob *et al.*, 2000; Murray, 2002). Each bacterium cell swims randomly in the fluid medium to locate the nutrient. In the average, the migration of bacterial cell is modeled as the diffusion. Bacteria consume nutrient and increase the numbers by cell division. When the nutrient is depleted, the bacteria die. The net rate of birth and death of bacteria is represented by the reaction term. The general form of reaction-diffusion equation, in

one-dimensional space, is given by (Murray, 2002)

$$\frac{\partial \rho}{\partial t} = \frac{\partial}{\partial x} \left( D \frac{\partial \rho}{\partial x} \right) + f(\rho), \quad (1)$$

where  $\rho(x, t)$  is bacterial population density at position  $x$  and time  $t$ ,  $D$  is diffusion coefficient and  $f(\rho)$  is reaction term. Here  $\rho(x, t) \geq 0$ . The most recognized model is the Fisher equation, which has been originated for the description of the spreading of mutant gene in a population (Fisher, 1937). In the Fisher model, the diffusion coefficient is constant,  $D = k$ , and the reaction term is the logistic growth law. The Fisher equation is given by

$$\frac{\partial \rho}{\partial t} = k \frac{\partial^2 \rho}{\partial x^2} + \alpha \rho \left( 1 - \frac{\rho}{\rho_M} \right), \quad (2)$$

where  $\alpha$  is rate constant and  $\rho_M$  is maximum density (Murray, 2002). We note that the logistic law in (2) describes the rate of population change under the limited resources (Fisher, 1937; Murray, 2002). The density cannot be greater than the maximum value  $\rho_M$ . Therefore the density is limited to  $0 \leq \rho \leq \rho_M$ . The solution to the Fisher equation (2) has demonstrated the propagation of the population density as the smooth traveling wave of form  $u(x - ct)$  with constant front speed,  $c \geq 2\sqrt{k\alpha}$  (Murray, 2002). This illuminates that the populations evolve with the well-defined pattern formations. Inspired by this, the study on pattern formation in the reaction-diffusion model has been attractive. Due to the diffusion coefficient is constant, the Fisher model describes the migration of the individual member of bacterial cell as the purely random walk. However, the random walk is unrealistic motion of the biological organism, which has sense. Gurney and Nisbet have proposed that the biological organisms move in such the way that they avoid the crowded population (Gurney and Nisbet, 1975). In this manner, they move in the direction of decreasing population density as fast as the population density is increasing. In this case, the diffusion coefficient linearly depends on the population density:  $D(\rho) = k(\rho / \rho_M)$ , where  $k$  is constant. Later, Gurtin and MacCamy have proposed a general form of diffusion coefficient:  $D(\rho) = k(\rho / \rho_M)^q$ , where  $q > 0$  and it implies the degree of population pressure (Gurtin and MacCamy, 1977). Newman has also found a general form of logistic law:

$f(\rho) = \alpha\rho \left[ 1 - (\rho / \rho_M)^q \right]$  (Newman 1983). Consequently, the density-dependent reaction-diffusion equation or the generalized Fisher equation have been originated:

$$\frac{\partial \rho}{\partial t} = k \frac{\partial}{\partial x} \left[ \left( \frac{\rho}{\rho_M} \right)^q \frac{\partial \rho}{\partial x} \right] + \alpha \rho \left[ 1 - \left( \frac{\rho}{\rho_M} \right)^q \right]. \quad (3)$$

Newman has found that the solution to (3) is the sharp traveling wave with the constant front speed,  $c = \sqrt{k\alpha / (q+1)}$  (Newman, 1980, 1983; Murray, 2002).

In our previous work, we have found a general form of the exact solution to (3) (Ngamsaad and Khompurngson, 2012a). The solution evolves from a specific initial state and converge to the sharp traveling wave of Newman's solution (Newman, 1983) with constant front speed at the long time and large distance. In addition, we have also found the exact solution for (3) by including the chemotaxis, the movement in responding to chemical gradient (Ngamsaad and Khompurngson, 2012b). However, as we introduced, the conventional model does not deal with the shape effect of the bacterial cell. The bacteria are the rod-shaped organisms, not the ideal point-like particle. The expansion of their colony should be influenced by the cell-to-cell interaction.

### 3. Model

Based on the experimental evidences, the shape of bacteria involves the cell ordering and clustering in the colony (Volfson *et al.*, 2008; Zhang *et al.*, 2010). Recently, it has been observed that the expansion of the bacterial colony is caused by cell pushing rather than by cell migration (Su *et al.*, 2012). Therefore, the effect of the mechanical interaction could dominate the diffusion. The biomechanical models have been proposed for the investigating the pattern formation in bacterial colony (Volfson *et al.*, 2008; Farrell *et al.*, 2013). Their model are formulated by the coupled nonlinear hydrodynamic equations and the reaction-diffusion equations. The governing equations in the model of Farrell *et al.* are of interest, which the mechanical interaction can be contributed to the model via the pressure (Farrell *et al.*, 2013).

In our approach, the bacterial populations are viewed as the continuum fluid that flows and reproduces to increase the cell numbers. The dynamics of system is governed by the continuity equation (Murray, 2002)

$$\frac{\partial \rho}{\partial t} + \frac{\partial}{\partial x} (\rho v) = g(\rho), \quad (4)$$

where  $v(x, t)$  is the local velocity of the bacterial population and  $g(\rho)$  describes the net rate of growth and death of bacteria. As usual, the net rate of the growth and death obeys the logistic law. Imagine that, the bacteria are growing in the dense colony and the number of cells are increasing by cell division. The flow of the bacterial population is driven by the gradient of internal pressure  $p(\rho)$ . When a bacterium tries to move, it collides with the surrounding cells. In this scenario, the velocity of the bacteria is strongly slowed down by the mechanical friction force  $-\gamma v$ . Balancing this two forces, we arise

$$-\gamma v = \frac{\partial}{\partial x} p(\rho), \quad (5)$$

where  $\gamma$  is friction constant. Equation (5) is similar to the Darcy's law that describes the fluid flow in porous media.

In our model, the bacterial cells are hard elastic rods in one-dimensional space, which consists of non-overlapping line segment of average length  $\sigma$ . This system is known as the Tonks' gas, which the pressure (or equation of state) is provided by

$$p(\rho) = k_B T \frac{\rho}{1 - \rho\sigma}, \quad (6)$$

where  $k_B$  is Boltzmann constant and  $T$  is temperature (Tonks, 1936). We note that, in one-dimensional space, the density means the numbers per unit length and the pressure is force per unit length or line tension. The bacterial colony is grown under the constant temperature (or isothermal condition) thus  $T$  is constant. Combining (4), (5) and (6), we arise the nonlinear partial differential equation

$$\frac{\partial \rho}{\partial t} = k \frac{\partial}{\partial x} \left[ \rho \frac{\partial}{\partial x} \left( \frac{\rho}{1 - \rho\sigma} \right) \right] + \alpha \rho \left( 1 - \frac{\rho}{\rho_M} \right), \quad (7)$$

where  $k = k_B T / \gamma$ . Equation (7) is still called the reaction-diffusion equation but it incorporates the shape effect of bacterial cell through the factor  $(1 - \rho\sigma)^{-1}$ . This factor goes to infinity for  $\rho \rightarrow 1/\sigma$ . Therefore, the maximum density is as  $\rho_M = 1/\sigma_M$  where  $\sigma_M < \sigma$ . Physically, it means one cell can occupy the region with length that is equal to  $\sigma_M$  maximally. This limits the density to  $0 < \rho < \rho_M$ . If the shape does not matter, by setting cell length to zero ( $\sigma = 0$ ), equation (7) recovers the conventional model (3) for  $q = 1$  equivalently. The exact solution in this case has been found from our previous work (Ngamsaad and Khompurngson, 2012a).

## 4. Results and Discussion

In this section, we briefly discuss the main results that we have found in this research. To avoid replication of our published paper (Ngamsaad and Suantai, 2016), the full details for technical calculations are omitted and listed in that paper in the Appendix, instead.

### 4.1 Analytical solutions

For convenience in further analysis, we introduce the dimensionless quantities:

$u = \rho / \rho_m$ ,  $\varepsilon = \sigma \rho_m = \sigma / \sigma_m$ ,  $t' = \alpha t$  and  $x' = \sqrt{\gamma \alpha \sigma / (k_B T)} x$ . Thus  $\varepsilon$  is called the packing fraction. Applying these quantities to (7), we obtain the dimensionless reaction-diffusion equation

$$\frac{\partial u}{\partial t'} = \frac{\partial}{\partial x'} \left[ \frac{u}{(1 - \varepsilon u)^2} \frac{\partial u}{\partial x'} \right] + u(1 - u), \quad (8)$$

where the unknown parameters have been hidden. Now the dimensionless density is limited to  $0 \leq u < 1$ . At the initial state, the density is low, thus  $\varepsilon \ll 1$ . This condition should provide the analytical solution to (8) by using the same analysis as our previous work (Ngamsaad and Khompurngson, 2012a). Here, we focus on the travelling solution of (8) that is  $u(x', t') = \phi(z)$  and  $z = x' - ct'$  where  $c$  is the wave speed. From (8), we have

$$\frac{d}{dz} \left[ \frac{\phi}{(1 - \varepsilon \phi)^2} \frac{d\phi}{dz} \right] + c \frac{d\phi}{dz} + \phi(1 - \phi) = 0. \quad (9)$$

The analytical solution of (9) can be obtained by using the perturbation method as described in our published paper (Ngamsaad and Suantai, 2016). From the analytical solution, the density profile is given by

$$\phi(z) = \begin{cases} \frac{1 - \exp[b(z - z_0)]}{1 - a \exp[b(z - z_0)]}, & z \leq z_0 \\ 0, & z > z_0, \end{cases} \quad (10)$$

where  $a = \frac{6\varepsilon}{5 + 2\varepsilon}$ ,  $b = \frac{5 - 4\varepsilon}{5\sqrt{2}}$ , and  $z_0$  is initial front position. Moreover, we obtain the

analytical form of the front speed (Ngamsaad and Suantai, 2016)

$$c(\varepsilon) = \frac{5}{\sqrt{2\varepsilon}} \frac{(4\varepsilon - 6)\ln(1 - \varepsilon) + \varepsilon^2 - 6\varepsilon}{(2\varepsilon^2 - 11\varepsilon + 8)\ln(1 - \varepsilon) - 7\varepsilon^2 + 8\varepsilon}. \quad (11)$$

From (11), we see that the front speed is dependence on the packing fraction  $\varepsilon$ .

## 4.2 Numerical solutions

To see the actual dynamics of the model, we have solved the full equation (8) by using a nonstandard fully implicit finite-difference method as described in our published paper (Ngamsaad and Suantai, 2016). We define the discrete density as  $u_j^n = u(x_j, t_n)$  where  $x_j = j\delta x$ ,  $t_n = n\delta t$ ,  $\delta x$  is grid spacing and  $\delta t$  is time step. Then, equation (8) in the discrete form is given by

$$\frac{\partial u_j^{n+1}}{\partial t'} = \frac{\partial}{\partial x'} \left[ M_j^n \frac{\partial u_j^{n+1}}{\partial x'} \right] + f_j^n u_j^{n+1}, \quad (12)$$

where  $M_j^n = u_j^n / (1 - \epsilon u_j^n)^2$  and  $f_j^n = 1 - u_j^n$ . Equation (12) can be discretized further

$$\frac{u_j^{n+1} - u_j^n}{\delta t} = \frac{1}{(\delta x)^2} \left[ M_{j+1/2}^n (u_{j+1}^{n+1} - u_j^{n+1}) - M_{j-1/2}^n (u_j^{n+1} - u_{j-1}^{n+1}) \right] + f_j^n u_j^{n+1}, \quad (13)$$

where  $M_{j\pm 1/2}^n = (M_{j\pm 1}^n + M_j^n) / 2$ . The complete algorithm is provided in our published paper (Ngamsaad and Suantai, 2016), listed in the Appendix.

Now, we show the results obtained from the numerical method. We have studied the dynamics of our model by varying the fraction for 0 to 0.999999. The demonstration of bacterial density profile is shown in Fig. 1. It was observed that the density profile evolved with the sharp traveling wave with unchanged shape.

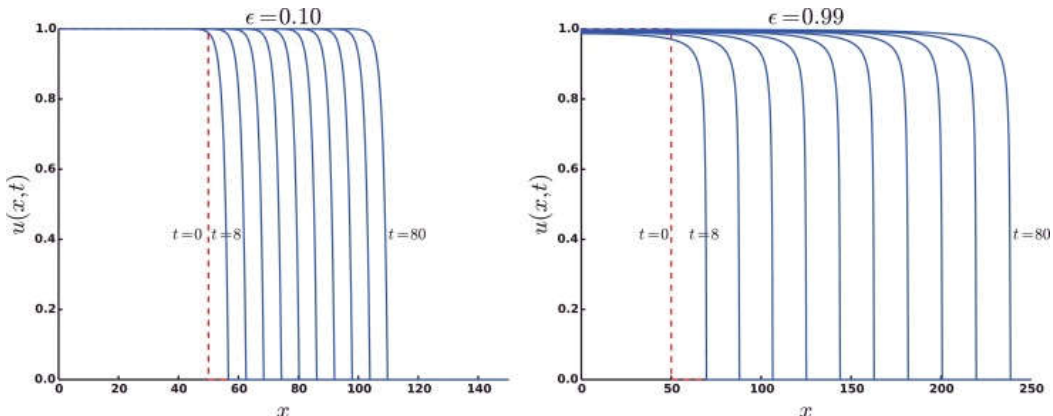


Fig. 1: The demonstration of density profiles, evolving from  $t=0$  to  $t=80$ , obtained by using the numerical method. The dashed lines represent the initial density profiles. The data are shown for every  $t=8$ .

We also measured the front speed directly from the numerical results. The front speed by varying the packing fraction is plotted in Fig. 2 in comparison with the analytical solution in (11). We found that the front speed increased with the packing fraction and reached a finite value as  $\epsilon \rightarrow \infty$ . The analytical results agreed with the numerical data for the small packing fraction.

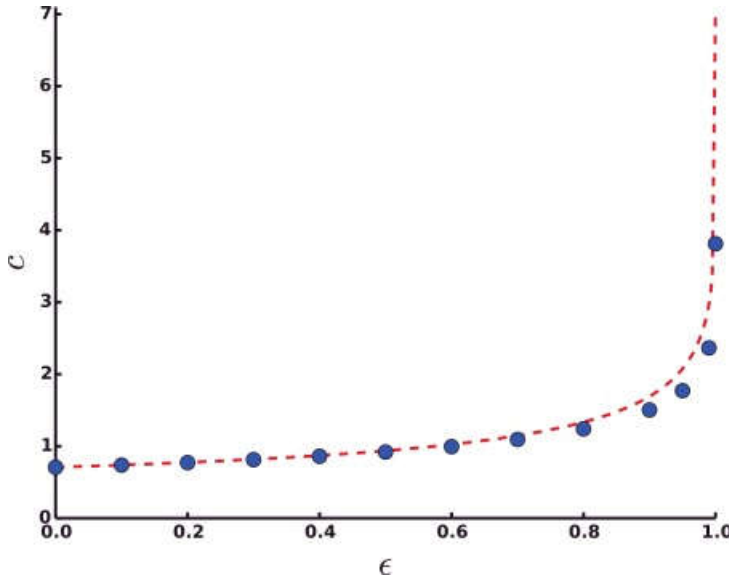


Fig. 2: The front speed versus the packing fraction,  $\epsilon$ . The dashed line represents the analytical curve generated from (11) and the circle markers represent the numerical results.

#### 4.3 Comparison to the experimental results

Finally, we compared our theoretical results to experimental evidence. From the experiments (Sokolov, et al., 2007; Rabani, Ariel, and Be'er, 2013), the dependence upon the packing fraction of average (or typical) velocity in bacterial suspensions was determined. Below a critical packing fraction  $<1$ , the average velocity of bacteria increased with the packing fraction and reached the maximum value at the critical packing fraction. Above this critical point, the average velocity decayed to zero as the packing fraction approached one, due to the lack of free space. The increased front speed relative to the packing fraction observed in our model qualitatively agrees with the experimental observations under the former conditions. Their observations under the latter conditions were not observed in our results, given that the front speed in our model reached the maximum value when the packing fraction equaled one, which represents the closest packing fraction for a one-dimensional hard-rod system.

#### 5. Concluding remarks

We have modified the reaction-diffusion model for bacterial population dynamics by incorporating the mechanical interaction between cells. The solutions of this model have been solved both analytically and numerically. The theoretical results revealed that the expansion speed of bacterial colonies was enhanced by the exclusion effect and

dependent upon the cell-packing fraction. These findings are qualitatively consistent with experimental evidence.

The solutions from this equation, both analytically and numerically, could provide better understanding of how the mechanical interactions control the structure and pattern formation of the bacterial colony. Precisely, it helps us to understand the spreading of bacterial density in space and time and the expansion speed of bacterial colony. Moreover, this simple one-dimensional model can be extended to investigate this problem in two-dimensional space for the future work.

### References

Ben-Jacob, E., Cohen, I. and Levine, H. (2000). Cooperative self-organization of microorganisms. *Adv. Phys.* 49 (4): 395-554.

Ben-Jacob, E., Coffey, D.S. and Levine, H. (2012). Bacterial survival strategies suggest rethinking cancer cooperativity. *Trends Microbiol.* 20 (9): 403-410.

Farrell, F.D.C., et al., (2013). Mechanically driven growth of quasi-two dimensional microbial colonies. *Phys. Rev. Lett.* 111: 168101.

Fisher, R. A. (1937). The wave of advance of advantageous genes. *Ann. Eugenics* 7(4): 355-369.

Golding, I., Kozlovsky, Y., Cohen, I., Ben-Jacob, E. (1998). Studies of bacterial branching growth using reaction-diffusion models for colonial development. *Physica A* 260 (3-4): 510-554.

Gurney, W. and Nisbet, R. (1975). The regulation of inhomogeneous populations. *J. Theor. Biol.* 52(2): 441-457.

Gurtin, M. E. and MacCamy, R. C. (1977). On the diffusion of biological populations. *Math. Biosci.* 33(1-2): 35-49.

Kawasaki, K., et al., (1997). Modeling spatio-temporal patterns generated by *Bacillus subtilis*. *J. Theor. Biol.* 188(2): 177-185.

Murray, J. (2002). *Mathematical Biology I: An Introduction*. New York: Springer.

Newman, W.I. (1980). Some exact solutions to a non-linear diffusion problem in population genetics and combustion. *J. Theor. Biol.* 85(2): 325-334.

Newman, W.I. (1983). The long-time behavior of the solution to a non-linear diffusion problem in population genetics and combustion. *J. Theor. Biol.* 104(4): 473-484.

Ngamsaad, W. and Khompurngson, K. (2012a). Self-similar solutions to a density-dependent reaction-diffusion model. *Phys. Rev. E* 85(6): 066120.

Ngamsaad, W. and Khompurngson, K. (2012b). Self-similar dynamics of bacterial chemotaxis. *Phys. Rev. E* 86(6): 062901.

Ngamsaad, W. and Suantai, S. (2016). Mechanically-driven spreading of bacterial populations. *Commun. Nonlinear Sci. Numer. Simulat.* 35: 88-96.

Press, W. H., et al., (1988). Numerical recipes in C: The art of scientific computing. New York: Cambridge university press.

Rabani, A., Ariel, G. and Be'er, A. (2013). Collective motion of spherical bacteria. *PLoS ONE*, 8 (12): e83760.

Sokolov, A., et al., (2007). Concentration dependence of the collective dynamics of swimming bacteria. *Phys. Rev. Lett.* 98 (2007): 158102.

Su, P.-T., et al., (2012). Bacterial colony from two-dimensional division to three-dimensional development. *PLoS ONE* 7(11): e48098.

Tonks, L. (1936). The complete equation of state of one, two and three-dimensional gases of hard elastic spheres. *Phys. Rev.* 50: 955-963.

Wolfson, D., et al., (2008). Biomechanical ordering of dense cell populations. *Proc. Natl. Acad. Sci. USA* 105(40): 15346-15351.

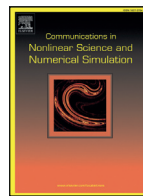
Zhang, H.P., et al., (2010). Collective motion and density fluctuations in bacterial colonies. *Proc. Natl. Acad. Sci. USA* 107(31): 13626-13630.

**Output จากโครงการวิจัยที่ได้รับทุนจาก สกอ.**

1. ผลงานตีพิมพ์ในวารสารวิชาการนานาชาติ
  - **Ngamsaad, W.** and Suantai, S. (2016). Mechanically-driven spreading of bacterial populations. *Commun. Nonlinear Sci. Numer. Simulat.* 35: 88-96. (Impact factor 2014: **2.866**)
2. การนำผลงานวิจัยไปใช้ประโยชน์
  - เชิงวิชาการ

ปัญหาการกระจายตัวเชิงกลของประชากรแบคทีเรียที่เรียกว่ามาเป็นหัวข้อหนึ่งในการเรียนการสอนวิชาชีวพิสิกส์
3. อื่นๆ
  - การเสนอผลงานในที่ประชุมวิชาการ  
**Waipot Ngamsaad** and Suthep Suantai, “*Reaction-diffusion model for mechanically spreading of bacterial populations*” นำเสนอผลงานวิจัยโดยการบรรยายปากเปล่า โครงการสัมมนาวิจัยพื้นฐาน สกอ. TRF Seminar Series in Basic Research “Science Research & Thailand’s Competitiveness” วันที่ 31 สิงหาคม 2558 ณ ห้องสัมมนา ชั้น 1 สำนักบริการเทคโนโลยีสารสนเทศ มหาวิทยาลัยเชียงใหม่

# ภาคผนวก



## Mechanically-driven spreading of bacterial populations



Waipot Ngamsaad <sup>a,\*</sup>, Suthep Suantai <sup>b</sup>

<sup>a</sup> Division of Physics, School of Science, University of Phayao, Phayao 56000, Thailand

<sup>b</sup> Department of Mathematics, Faculty of Science, Chiang Mai University, Chiang Mai 50200, Thailand

### ARTICLE INFO

#### Article history:

Received 9 August 2015

Revised 1 October 2015

Accepted 20 October 2015

Available online 12 November 2015

#### Keywords:

Traveling wave

Nonlinear reaction-diffusion model

Bacterial colony

### ABSTRACT

The effect of mechanical interactions between cells in the spreading of bacterial populations was investigated in one-dimensional space. A continuum-mechanics approach, comprising cell migration, proliferation, and exclusion processes, was employed to elucidate the dynamics. The consequent nonlinear reaction-diffusion-like equation describes the constitution dynamics of a bacterial population. In this model, bacterial cells were treated as rod-like particles that interact with each other through hard-core repulsion, which introduces the exclusion effect that causes bacterial populations to migrate quickly at high density. The propagation of bacterial density as a traveling wave front over extended times was also analyzed. The analytical and numerical solutions revealed that the front speed was enhanced by the exclusion process, which depended upon the cell-packing fraction. Finally, we qualitatively compared our theoretical results with experimental evidence.

© 2015 Elsevier B.V. All rights reserved.

### 1. Introduction

In recent decades, much attention has been paid to the collective behavior of bacterial populations. This system is used as the prototype for understanding multicellular assemblies, such as tissue and biofilm [1]. The insight into the underlying mechanism of dynamics is important to biological and medical science.

To cope with unfavorable environmental conditions, bacterial colonies generate varieties of pattern formations [2,3]. The spatiotemporal pattern formation in bacterial colonies results from cell migration and proliferation. These dynamics at a continuum level can be described by reaction-diffusion processes [2–4]. The simplified model [2] relied on a density-dependent (or degenerate) reaction-diffusion equation [5–9], which was an extension of the classical Fisher-KPP equation [10,11]. These well-known solutions [7,8] revealed that bacterial density evolves as a sharp traveling wave with constant front speed [2]. In our previous work, we found an explicit space-time solution for the generalized Fisher-KPP equation in one-dimensional space [12]. This solution evolves from a specific initial condition to a self-similar object that converges to the usual traveling wave on an extended time scale. Although capable of explaining these dynamics, the conventional model omitted the size of the bacterial cell. In real systems, most bacterial cells are rod shaped and grow in dense environments. Accordingly, the mechanical interactions between cells could play crucial roles in the spreading of bacterial colonies.

Recent experimental and theoretical studies showed that mechanical interactions between cells have important roles in the collective behavior of bacterial colonies [13–18]. The dependence on the elastic modulus of the front speed has theoretically been found [19]. It mentions that *the migration of bacteria is caused by cell pushing rather than self-propulsion* in dense colonies [14,17,18]. Therefore, we speculate that the exclusion process that prevents the overlapping of cells could play a crucial role in

\* Corresponding author. Tel.: +6654466666.

E-mail addresses: [waipot.ng@up.ac.th](mailto:waipot.ng@up.ac.th) (W. Ngamsaad), [suthep.s@cmu.ac.th](mailto:suthep.s@cmu.ac.th) (S. Suantai).

the spreading of bacterial colonies. This issue motivates us to extend the conventional density-dependent reaction-diffusion equation [5–9] by incorporating the cell size into the investigation of the dynamics of bacterial populations.

In this work, we considered the systems of bacterial cells growing on a thin layer of nutrient-rich fluid medium. The bacteria increased in population through cell division and interacted through hard-core repulsion (steric interactions), which resulted in exclusion effects and consequent non-overlapping of cells. Although bacteria are self-propelled particles [20], in colonies of densely packed or non-motile cells, bacterial migration was caused by cell pushing, resulting from cell growth and division, rather than self-propulsion [14,17,18]. Thus, *the bacteria behave similarly as passive particles or non-motile cells* in high density environments. Apart from cells, Bruna and Chapman [21] observed that the self-diffusion of hard spherical Brownian particles in a dilute regime decreased as the density increased, due to the diffusion of any single particle being impeded by collisions with other particles. However, these collisions encouraged the particle to move toward low-density regions, resulting in this biased migration being faster than self-diffusion and enhancing overall collective diffusion. Guided by the work of Bruna and Chapman [21], we propose that bacterial cells move based on hard-core repulsion and without self-propelled motility in dense colonies.

After incorporating exclusion processes in cell (or particle) dynamics, altered diffusion coefficients in the continuum limits were found [22–29]. The enhancement or slowing of diffusion depends upon cell length and the available moving distance, as shown by lattice-based analysis [28]. In some models, diffusion diverges to infinity in closely packed densities [22,23,29]. Singular diffusion has also been modeled through the migration of bacterial biofilm [30,31] and glioblastoma tumors [32]. However, the effect of diverged diffusion on the propagation speed of cell populations remains unknown.

To address this question, we employed a continuum-mechanics approach to cell proliferation [33] in order to investigate the spreading of bacterial populations in the presence of exclusion processes. Additionally, we analytically and numerically elucidated the front speed of bacterial colony expansion in terms of cell size and discussed the consistency of our theoretical results with the experimental evidence.

## 2. Continuum mechanical model

### 2.1. Constitution equations

From a macroscopic view, bacterial populations constitute continuum fluid capable of reproducing in order to increase cell numbers. By pushing each other following cell division [14,17,18], population pressure increases as a result of collisions between cells and forces cells to move. During movement, cells encounter friction from the surrounding fluid medium and the substrate surface. For the sake of simplicity, we considered the expansion of bacterial colonies in one-dimensional space, regardless of cell orientation. Adapting from [33], the constitution equations that describe the evolution of the cell density,  $\rho(x, t)$ , and collective velocity,  $V(x, t)$ , of the bacterial population at position  $x$  and time  $t$  are given by

$$\frac{\partial \rho}{\partial t} = -\frac{\partial(\rho V)}{\partial x} + \Gamma(\rho), \quad (1)$$

$$-\gamma V = \frac{\partial p}{\partial x} = \frac{\partial p}{\partial \rho} \frac{\partial \rho}{\partial x}, \quad (2)$$

where  $\Gamma(\rho(x, t))$  represents the growth function,  $p(\rho(x, t))$  represents the internal population pressure, and  $\gamma$  represents the damping constant. Eq. (1) represents the continuity equation with the growth term. We assume that bacterial growth obeys the law of population growth as described by a logistic function:  $\Gamma(\rho) = \kappa \rho(1 - \rho/\rho_m)$ , where  $\kappa$  is the rate constant and  $\rho_m$  is the maximum density [9,33]. Eq. (2) arises from the force balance between Stokes' law for friction and the pressure gradient, which is similar to Darcy's law describing fluid flow through a porous medium.

We model the bacterial cells as non-overlapping hard-rod particles of average length,  $\sigma$ , that interact through hard-core repulsion. In high-density environments, bacterial self-propulsion can be ignored, since it is dominated by collision between cells. This defines the bacterial cell as a passive particle or non-motile cell that obeys the laws of thermodynamics. For hard-rod fluid in one dimension, the exact pressure is given as

$$p(\rho) = \frac{\rho k_B T}{1 - \sigma \rho}, \quad (3)$$

where  $k_B$  is the Boltzmann constant and  $T$  represents the temperature [34–36]. In our case where bacterial cells behave as passive particles, the temperature relates to the average translational kinetic energy of a cell,  $\langle E_k \rangle = (1/2)k_B T$ , we assume that the temperature is constant in our system. The pressure in Eq. (3) diverges to infinity at closely packed density:  $\rho \rightarrow 1/\sigma$ . Notably, in dilute density,  $\rho \rightarrow 0$ , Eq. (3) recovers the pressure of an ideal gas:  $p = \rho k_B T$ . As shown in [37–39], the pressure for dilute active particles is similar to the ideal gas, except that the source of kinetic energy comes from the swim speed,  $U_0$ :  $k_B T \propto U_0^2$  [37,38]. As will be shown later, the temperature source is not important; as long as it is constant, the dynamics of our model are invariant.

### 2.2. Dimensionless equations

We define the maximum density as  $\rho_m = 1/\sigma_m$ , where  $\sigma_m$  represents the average length occupied by one cell and  $\sigma_m > \sigma > 0$ . The logistic law limits the growth of bacteria, such that  $0 \leq \rho \leq \rho_m < 1/\sigma$ . For convenience of further analysis, we

introduce the following dimensionless quantities:  $0 \leq u = \rho/\rho_m \leq 1$ ,  $v = [\gamma/(\kappa \rho_m k_B T)]^{1/2} V$ ,  $0 < \epsilon = \sigma \rho_m = \sigma/\sigma_m < 1$ ,  $t' = \kappa t$ , and  $x' = [(\kappa \gamma)/(\rho_m k_B T)]^{1/2} x$ . In one dimension, the packing fraction, ( $\epsilon$ ), represents the length fraction, which is equivalent to the area and volume fractions in two and three dimensions, respectively. We then rewrite Eq. (1) and (2) by employing Eq. (3) in dimensionless form:

$$\frac{\partial u}{\partial t} = -\frac{\partial(uv)}{\partial x} + u(1-u), \quad (4)$$

$$v = -\frac{1}{(1-\epsilon u)^2} \frac{\partial u}{\partial x}, \quad (5)$$

where the prime has been dropped. From Eq. (5), the migration of bacterial populations is biased to move down the density gradient and enhanced by the exclusion process, implied from the factor  $1/(1-\epsilon u)^2$ . This factor increases with the density and diverges to infinity as  $\epsilon \rightarrow 1$  at  $u = 1$ , which causes the bacterial population to migrate faster at higher density. This singularity has appeared in similar models using different approaches [22,23,29–32,40]. Fortunately, the velocity in Eq. (5) is finite, since  $\partial u/\partial x \rightarrow 0$  at  $u = 1$ . The density inside of the colony reaches a saturated value, except in proximity to the colony edge. In this regime, the density distribution is homogeneous and its gradient approaches zero.

Substituting Eq. (5) into Eq. (4), we obtain a nonlinear partial differential equation:

$$\frac{\partial u}{\partial t} = \frac{\partial}{\partial x} \left( M(u) \frac{\partial u}{\partial x} \right) + g(u), \quad (6)$$

where  $M(u) = u/(1-\epsilon u)^2$  and  $g(u) = u(1-u)$ . Eq. (6) is in the same form as the density-dependent reaction-diffusion equation, however, the migration or diffusion coefficients differ. This is unrelated to the mean-square displacement, however,  $M \sim \rho \partial p / \partial \rho$ . In this model, the populations migrate based on the collision between cells as opposed to a random walk. A similar coefficient represents the contribution of hard-core repulsion between cells to the migration of myxobacteria in a dense phase [40]. Eq. (6) is degenerate based on  $M(0) = 0$ , which results in the sharp interface separated between occupied and cell-free regions. In a very dilute system ( $\epsilon \rightarrow 0$ ), Eq. (6) recovers the conventional degenerate Fisher-KPP equation [7–9], for which an explicit solution was determined in our previous work [12].

### 3. Traveling-wave solution

We focused on behavior of the system over extended times, during which the population density propagates as a traveling wave:  $u(x, t) = \phi(z)$ , where  $z = x - ct$  and  $c$  represent the front speed [9]. Substituting the traveling-wave solution into Eq. (6), we obtain

$$\frac{d}{dz} \left( M(\phi) \frac{d\phi}{dz} \right) + c \frac{d\phi}{dz} + g(\phi) = 0. \quad (7)$$

In the degenerate model, the density must vanish at the finite position,  $z^* (< \infty)$ , that undergoes the sharp interface. We then consider the density profile that satisfies the following conditions:  $\phi(-\infty) = 1$ ,  $\phi(z) = 0$  for  $z \geq z^*$ ,  $\frac{d}{dz} \phi(-\infty) = 0$ , and  $\frac{d}{dz} \phi(z^*) \neq 0$ . Additionally, for  $\epsilon \in [0, 1]$ ,  $M(\phi(-\infty)) < \infty$  and  $M(\phi(z)) = 0$  for  $z \geq z^*$  [41]. Multiplying Eq. (7) by  $M(\phi) d\phi/dz$  and then integrating with respect to  $z$  from  $-\infty$  to  $z^*$ , we obtain  $c \int_{-\infty}^{z^*} M(\phi) \left( \frac{d\phi}{dz} \right)^2 dz + \int_{-\infty}^{z^*} M(\phi) g(\phi) \frac{d\phi}{dz} dz + \frac{1}{2} (M(\phi) \frac{d\phi}{dz})^2 \Big|_{-\infty}^{z^*} = 0$ . Under these density profile conditions, the last term on the left-hand side is zero. Finally, we obtain the front speed:

$$c = -\frac{\int_0^1 M(\phi) g(\phi) d\phi}{\int_0^1 M(\phi) \left( \frac{d\phi}{dz} \right) d\phi}. \quad (8)$$

To obtain the closed-form of the front speed,  $c$ , the solution for the density gradient,  $d\phi/dz$ , is required.

#### 3.1. Approximate solution

Although the exact solution of Eq. (7) remains unknown, we can find the approximate solution by employing the perturbation method [42]. By defining  $w(\phi) = d\phi/dz$ , we rewrite Eq. (7):

$$M(\phi) w \frac{dw}{d\phi} + M'(\phi) w^2 + cw + g(\phi) = 0, \quad (9)$$

where  $M'(\phi) = dM(\phi)/d\phi$ . The migration coefficient can be written in the expansion form:  $M(\phi) \approx \phi(1 + 2\phi\epsilon + 3\phi^2\epsilon^2 + \dots)$ . We then look for the solution of Eq. (9) in the power series of  $\epsilon$ :

$$w(\phi) = w_0(\phi) + w_1(\phi)\epsilon + w_2(\phi)\epsilon^2 + \dots, \quad (10)$$

$$c = c_0 + c_1\epsilon + c_2\epsilon^2 + \dots, \quad (11)$$

where  $w_i(\phi)$  and  $c_i$ , that  $i \in \{0, 1, 2, \dots, \infty\}$  are coefficients to be determined. Substituting Eq. (10) and (11) into Eq. (9), we obtain the equation for each order as follows: at  $\epsilon^0$ ,

$$\phi w_0 \frac{dw_0}{d\phi} + w_0^2 + c_0 w_0 + \phi(1 - \phi) = 0, \quad (12)$$

and, at  $\epsilon^1$ ,

$$\phi w_0 \frac{dw_1}{d\phi} + \left( \phi \frac{dw_0}{d\phi} + 2w_0 + c_0 \right) w_1 + 2\phi^2 w_0 \frac{dw_0}{d\phi} + 4\phi w_0^2 + c_1 w_0 = 0. \quad (13)$$

Eq. (12) has the known solutions:  $w_0 = (1/\sqrt{2})(\phi - 1)$  and  $c_0 = 1/\sqrt{2}$  [7–9,42]. Substituting these solutions into Eq. (13), we obtain a linear first-order ordinary differential equation:

$$\phi(\phi - 1) \frac{dw_1}{d\phi} + (3\phi - 1)w_1 + 3\sqrt{2}\phi^3 - 5\sqrt{2}\phi^2 + (2\sqrt{2} + c_1)\phi - c_1 = 0. \quad (14)$$

After finding the integrating factor [43], we obtain its solution:

$$w_1(\phi) = \frac{1}{(\phi - 1)^2} \left[ \frac{C}{\phi} - \frac{3\sqrt{2}}{5} \phi^4 + 2\sqrt{2}\phi^3 - \left( \frac{c_1}{3} + \frac{7\sqrt{2}}{3} \right) \phi^2 + (c_1 + \sqrt{2})\phi - c_1 \right], \quad (15)$$

where  $C$  is the integral constant. To prevent the singularity at  $\phi = 0$  and  $\phi = 1$ , we require that  $C = 0$  and  $-\frac{3\sqrt{2}}{5} + 2\sqrt{2} - (\frac{c_1}{3} + \frac{7\sqrt{2}}{3}) + (c_1 + \sqrt{2}) - c_1 = 0$ . Thus, we obtain

$$c_1 = \frac{2}{5\sqrt{2}}. \quad (16)$$

Substituting Eq. (16) into Eq. (15), we obtain

$$w_1(\phi) = -\frac{2}{5\sqrt{2}}(\phi - 1)(3\phi - 1). \quad (17)$$

Finally, gathering all terms, we obtain the approximate solutions with the correction of  $O(\epsilon^2)$

$$w = \frac{d\phi}{dz} = \frac{6(\phi - 1)}{5\sqrt{2}} \left( \frac{5 + 2\epsilon}{6} - \epsilon\phi \right) + O(\epsilon^2), \quad (18)$$

$$c = \frac{1}{\sqrt{2}} \left( 1 + \frac{2}{5}\epsilon \right) + O(\epsilon^2). \quad (19)$$

The density gradient approaches zero when the density reaches the maximum value,  $\phi \rightarrow 1$ , as expected. By using  $w(\phi) = d\phi/dz$ , we can calculate the approximate density profile:

$$\phi(z) = \begin{cases} \frac{1 - \exp[b(z - z_0)]}{1 - a \exp[b(z - z_0)]}, & z \leq z_0 \\ 0, & z > z_0, \end{cases} \quad (20)$$

where  $a = \frac{6\epsilon}{5 + 2\epsilon}$ ,  $b = \frac{5 - 4\epsilon}{5\sqrt{2}}$ , and  $z_0$  represents the initial front position where  $\phi(z_0) = 0$ .

### 3.2. Front speed

The front speed is the collective velocity at the edge of the colony,  $c = v(\phi(z^*)) = v(0)$ . Based on the correction of  $O(\epsilon^2)$  from Eq. (19), the front speed increases linearly with packing fraction ( $\epsilon$ ). However, substituting Eq. (18) into Eq. (8) and after integration, we can obtain a more precise front speed:

$$c(\epsilon) = \frac{5}{\sqrt{2}\epsilon} \frac{(4\epsilon - 6) \ln(1 - \epsilon) + \epsilon^2 - 6\epsilon}{(2\epsilon^2 - 11\epsilon + 8) \ln(1 - \epsilon) - 7\epsilon^2 + 8\epsilon}. \quad (21)$$

The front speed depends upon the packing fraction of a cell. Therefore, the front speed recovers the usual value, that  $c_0 = 1/\sqrt{2} \approx 0.7071$ , in a very dilute regime, as  $\epsilon \rightarrow 0$  [7–9,42]. In a closely packed regime, as  $\epsilon \rightarrow 1$ , the front speed approaches a finite value, that  $c(1) = 10/\sqrt{2} \approx 7.071$ , and increases by a factor of 10 from the dilute regime.

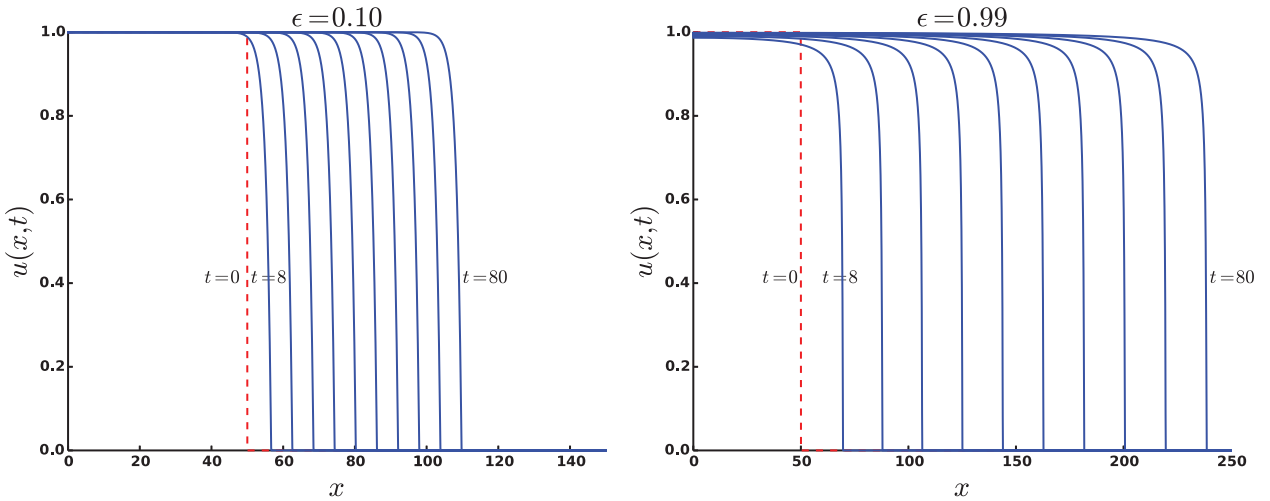


**Fig. 1.** The demonstration of density profiles,  $u(x, t)$ , evolving from  $t = 0$  to  $t = 80$ , obtained by using the numerical method. The dashed lines represent the initial density profiles. The data are shown for every  $t = 8$ . (For interpretation of the references to color in this figure legend, the reader is referred to the web version of this article).

#### 4. Numerical results and discussion

As the correction of our approximate solutions is limited to  $O(\epsilon^2)$ , it is counterintuitive, given that the model is designed for capturing dynamics at high density. To obtain the actual results at high density, we solved Eq. (6) directly and subjected the solution to a zero-flux boundary condition using the numerical method. In Eq. (6), the migration coefficient increases with density, which is inefficient when solving with an explicit finite-difference scheme [44]. Unfortunately, solving with the standard implicit-numerical scheme is also difficult because of the factor  $1/(1 - \epsilon u)^2$ . We found that the simplest algorithm that overcomes these obstructions is the nonstandard fully implicit finite-difference method [30]. This algorithm has proven stable enough to explore the dynamics at high-packing fractions. The detailed algorithm is described in the Appendix.

Although our model is not expected to be accurate for dilute systems, since it has neglected bacterial self-propulsion, we focused on bacterial population dynamics by varying the values of the packing fraction,  $\epsilon \in [0, 1]$ . For our computation, we chose the spacing step and the time step, such that  $\delta x = 0.05$  and  $\delta t = 0.01$ , respectively. The computations were performed on 3,000 grids for  $\epsilon \in [0, 0.5]$  and on 5,000 grids for  $\epsilon \in (0.5, 0.99]$ , with 8,000 iterations. For  $\epsilon = 0.999999$ , the computation was performed on 120,000 grids with 150,000 iterations. The initial density profile,  $u_0(x)$ , was set to a step function:

$$u_0(x) = \begin{cases} 1, & x < r_0 \\ 0, & x \geq r_0, \end{cases} \quad (22)$$

where  $r_0$  represents the initial front position. To ensure that it was far enough from the boundary at origin, we set  $r_0 = 50$ .

The demonstration of the density profiles, obtained from the numerical method, is shown in Fig. (1) for dilute systems ( $\epsilon = 0.10$ ) and dense systems ( $\epsilon = 0.99$ ). It was observed that the density profile evolved with the sharp traveling wave with unchanged shape. The front position,  $r_f(t)$ , was determined by the first position where the density fell to zero. Due to numerical deviation, we measured the first position where the density was  $1 \times 10^{-6}$ , or  $u(r_f, t) \leq 1 \times 10^{-6}$ . The front positions were collected for every  $t = 1$ . To avoid the transient effects of the initial stage, the last 50 data points were selected for fitting with the linear equation,  $r_f = ct + r_0$ . The corresponding front positions of the density profiles in Fig. (1), as a function of time, were fitted well using the linear equation, as demonstrated in Fig. (2). This implied that the density propagated with constant front speed, which was equal to the slope of the linear equation. We checked the accuracy of our algorithm by considering the front speed under conditions of  $\epsilon = 0$ . In this case, the numerical front speed was equal to 0.7074, which displayed an error of 0.04% of the exact value ( $c_0 = 1/\sqrt{2} \approx 0.7071$  [7–9,42]). Finally, we explored the dynamics of bacterial populations in a closely packed regime. We set  $\epsilon = 0.999999$ , in order to avoid dividing by zero for the factor  $1/(1 - \epsilon u)^2$  when  $u = 1$ . In a closely packed system, the numerical front speed was equal to 3.8115, which was less than the analytically predicted value due to the inaccuracy of the approximate solution. The plot of the numerical front speed versus the packing fraction, as compared with the analytical curve generated from Eq. (21), is shown in Fig. (3). We found that the front speed increased with the packing fraction and reached a finite value as  $\epsilon \rightarrow 1$ . The analytical results agreed with the numerical data for the small packing fraction ( $\epsilon \ll 1$ ), since the correction of our analytical solution was only  $O(\epsilon^2)$ .

Finally, we compared our theoretical results to experimental evidence. From the experiments [45,46], the dependence upon the packing fraction of average (or typical) velocity in bacterial suspensions was determined. Below a critical packing fraction  $< 1$ , the average velocity of bacteria increased with the packing fraction and reached the maximum value at the critical packing fraction [45,46]. Above this critical point, the average velocity decayed to zero as the packing fraction approached one, due to

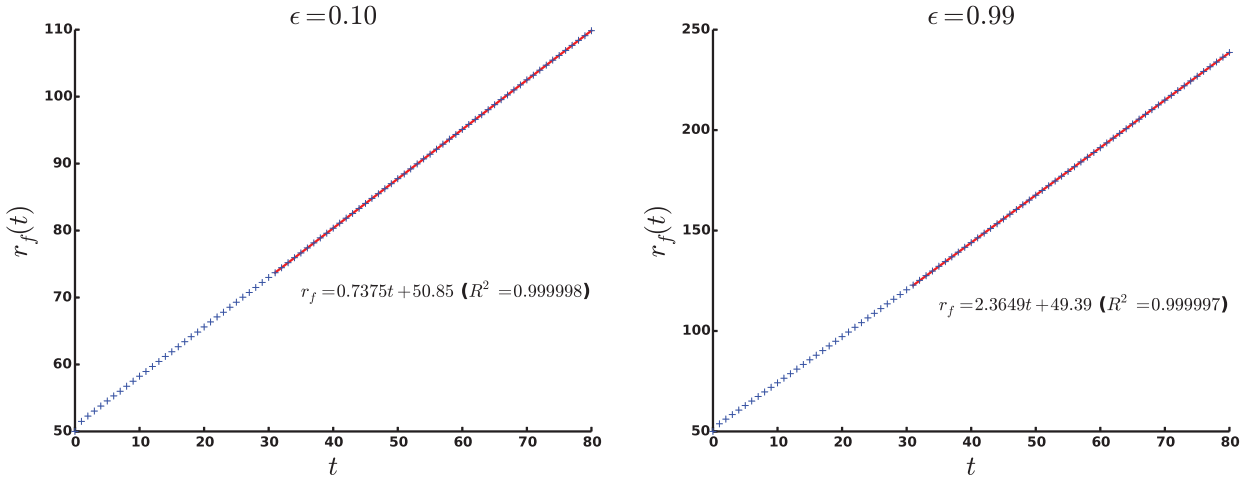


**Fig. 2.** The front position versus time, corresponding to the numerical density profiles in Fig. (1), from  $t = 0$  to  $t = 80$ . The data are shown for every  $t = 1$ . The markers represent numerical values and the solid lines represent the fitting lines for the last 50 data points.  $R^2$  is the correlation coefficient. (For interpretation of the references to color in this figure legend, the reader is referred to the web version of this article).

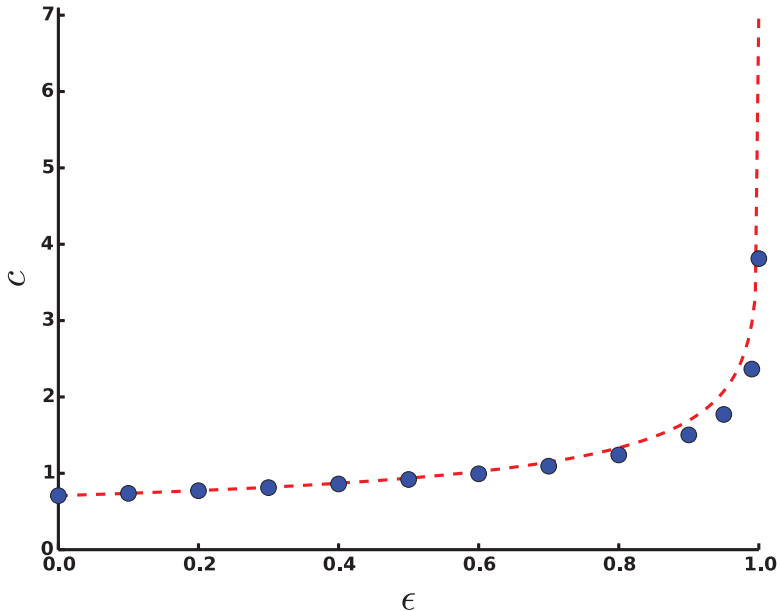


**Fig. 3.** The front speed versus the packing fraction,  $\epsilon$ . The dashed line represents the analytical curve generated from Eq. (21) and the circle markers represent the numerical results. (For interpretation of the references to color in this figure legend, the reader is referred to the web version of this article).

the lack of free space. The increased front speed relative to the packing fraction observed in our model qualitatively agrees with the experimental observations under the former conditions. Their observations under the latter conditions were not observed in our results, given that the front speed in our model reached the maximum value when the packing fraction equaled one, which represents the closest packing fraction for a one-dimensional hard-rod system. Nevertheless, our data showed that the numerical front speed in a closely packed regime increased by a factor of  $\sim 5$  relative to the dilute regime, which qualitatively agrees with experimental observations [45,46] showing increases in average velocity by a factor of  $\sim 3$  in suspensions of spherical-shaped bacteria [46] and in typical velocity by a factor of  $\sim 5$  in suspensions of rod-shaped bacteria [45].

## 5. Conclusion

This study demonstrated the effect of mechanical interactions between cells based on the spreading of bacterial populations by employing a continuum-mechanics modeling approach. In dense colonies, bacterial migration is dominated by hard-core repulsion between cells, which causes exclusion processes. The analytical and numerical results revealed that the expansion

speed of bacterial colonies was enhanced by the exclusion effect and dependent upon the cell-packing fraction. These findings are qualitatively consistent with experimental evidence.

## Acknowledgment

This research was supported by the TRF Grant for New Researchers (Grant no. TRG5780037), funded by The Thailand Research Fund and University of Phayao.

## Appendix A. Nonstandard fully implicit finite-difference scheme

We define the discrete density as  $u_j^n = u(x_j, t_n)$ , where  $x_j = j\delta x$ ,  $t_n = n\delta t$ ,  $\delta x$  is a spacing step,  $\delta t$  is a time step,  $j \in \{0, 1, 2, \dots, J\}$ ,  $n \in \{0, 1, 2, \dots, N\}$ , and  $J$  and  $N$  are integers. We then rewrite Eq. (6) as

$$\frac{\partial u_j^{n+1}}{\partial t} \approx \frac{\partial}{\partial x} \left( M_j^n \frac{\partial u_j^{n+1}}{\partial x} \right) + f_j^n u_j^{n+1}, \quad (\text{A.1})$$

where  $M_j^n = M(u_j^n) = u_j^n / (1 - \epsilon u_j^n)^2$  and  $f_j^n = 1 - u_j^n$ . Using the standard discretized scheme for the differential operators, we obtain

$$\frac{u_j^{n+1} - u_j^n}{\delta t} = \frac{1}{\delta x} \left( M_{j+1/2}^n \frac{\partial}{\partial x} u_{j+1/2}^{n+1} - M_{j-1/2}^n \frac{\partial}{\partial x} u_{j-1/2}^{n+1} \right) + f_j^n u_j^{n+1}. \quad (\text{A.2})$$

We discretize the remain gradient terms in Eq. (A.2) and then have

$$\frac{u_j^{n+1} - u_j^n}{\delta t} = \frac{1}{(\delta x)^2} \left[ M_{j+1/2}^n (u_{j+1}^{n+1} - u_j^{n+1}) - M_{j-1/2}^n (u_j^{n+1} - u_{j-1}^{n+1}) \right] + f_j^n u_j^{n+1}. \quad (\text{A.3})$$

The migration coefficient at the mid-grid can be computed by

$$M_{j-1/2}^n = \frac{1}{2} (M_{j-1}^n + M_j^n), \quad (\text{A.4})$$

$$M_{j+1/2}^n = \frac{1}{2} (M_j^n + M_{j+1}^n). \quad (\text{A.5})$$

Noting that the correction of Eq. (A.3) is  $O(\delta t, (\delta x)^2)$ . After rearranging Eq. (A.3), we have

$$\alpha_j^n u_{j-1}^{n+1} + \theta_j^n u_j^{n+1} + \beta_j^n u_{j+1}^{n+1} = u_j^n, \quad (\text{A.6})$$

where

$$\begin{aligned} \alpha_j^n &= -\mu M_{j-1/2}^n, \\ \beta_j^n &= -\mu M_{j+1/2}^n, \\ \theta_j^n &= 1 - \delta t f_j^n + \mu (M_{j-1/2}^n + M_{j+1/2}^n), \\ \mu &= \delta t / (\delta x)^2. \end{aligned} \quad (\text{A.7})$$

We impose the zero-flux condition at the boundary grid, saying  $\Omega$ , that  $\frac{\partial u}{\partial x} \Big|_{\Omega} = 0$  or  $\frac{u_{\Omega+1}^n - u_{\Omega-1}^n}{2\delta x} = 0$ . Consequently,  $u_{\Omega-1}^n = u_{\Omega+1}^n$  and  $M_{\Omega-1/2}^n = M_{\Omega+1/2}^n$ . We then rewrite Eq. (A.6), subjected to the zero-flux boundary condition, in matrix form:

$$\mathbf{A}^n \cdot \mathbf{U}^{n+1} = \mathbf{U}^n, \quad (\text{A.8})$$

where

$$\mathbf{A}^n = \begin{bmatrix} \theta_0^n & 2\beta_0^n & \cdots & \cdots & 0 \\ \alpha_1^n & \theta_1^n & \beta_1^n & & \vdots \\ \vdots & \ddots & \ddots & \ddots & \vdots \\ \vdots & & \alpha_{J-1}^n & \theta_{J-1}^n & \beta_{J-1}^n \\ 0 & \cdots & \cdots & 2\alpha_J^n & \theta_J^n \end{bmatrix}, \quad (\text{A.9})$$

and

$$\mathbf{U}^n = [ u_0^n \quad u_1^n \quad u_2^n \quad \cdots \quad u_J^n ]^T. \quad (\text{A.10})$$

According to the boundary condition,  $\theta_0^n = 1 - \delta t f_0^n + 2\mu M_{1/2}^n$  and  $\theta_j^n = 1 - \delta t f_j^n + 2\mu M_{j-1/2}^n$ . The numerical density is obtained by solving the matrix equation (Eq. (A.8)) iteratively.

To find the stability condition of this numerical scheme, we use von Neumann stability analysis:

$$u_j^n = (\lambda)^n e^{ikj\delta x}, \quad (\text{A.11})$$

where  $\lambda$  represents the amplification factor and  $k$  is the wave number [44]. Substituting Eq. (A.11) into Eq. (A.3), we obtain  $\lambda^{-1} = 1 - \delta t f_j^n - \mu M_{j+1/2}^n (e^{ik\delta x} - 1) + \mu M_{j-1/2}^n (1 - e^{-ik\delta x})$ , which can be approximated further:

$$\lambda \approx [1 - \delta t f_j^n + 4\mu M_j^n \sin^2(k\delta x/2) + O(\delta x)]^{-1}. \quad (\text{A.12})$$

A stable and temporal non-oscillated numerical solution requires that  $0 < \lambda \leq 1$  [30]. According to  $0 \leq f_j^n \leq 1$  and  $0 \leq M_j^n < \infty$ , without the growth term,  $(f_j^n)$ , this algorithm is unconditionally stable as long as  $\delta x \ll 1$  [44]. With the growth term, the solution slowly grows to a finite value as long as  $\delta t \ll 1$ . Based on Eq. (A.12), this algorithm is adequately stable for this type of problem.

## References

- [1] Shapiro JA. Thinking about bacterial populations as multicellular organisms. *Annu Rev Microbiol* 1998;52(1):81–104. doi:10.1146/annurev.micro.52.1.81.
- [2] Kawasaki K, Mochizuki A, Matsushita M, Umeda T, Shigesada N. Modeling spatio-temporal patterns generated by bacillus subtilis. *J Theor Biol* 1997;188(2):177–85.
- [3] Ben-Jacob E, Cohen I, Levine H. Cooperative self-organization of microorganisms. *Adv Phys* 2000;49:395–554.
- [4] Golding I, Kozlovsky Y, Cohen I, Ben-Jacob E. Studies of bacterial branching growth using reaction-diffusion models for colonial development. *Physica A* 1998;260(3–4):510–54.
- [5] Gurney W, Nisbet R. The regulation of inhomogeneous populations. *J Theor Biol* 1975;52(2):441–57.
- [6] Gurtin M, MacCamy R. On the diffusion of biological populations. *Math Biosci* 1977;33(1–2):35–49.
- [7] Newman W. Some exact solutions to a non-linear diffusion problem in population genetics and combustion. *J Theor Biol* 1980;85(2):325–34.
- [8] Newman W. The long-time behavior of the solution to a non-linear diffusion problem in population genetics and combustion. *J Theor Biol* 1983;104(4):473–84.
- [9] Murray J. Mathematical biology. New York: Springer-Verlag; 1989.
- [10] Fisher R. The wave of advance of advantageous genes. *Ann Eugen* 1937;7(4):355–69.
- [11] Kolmogorov A, Petrovskii I, Piscounov N. A study of the diffusion equation with increase in the amount of substance, and its application to a biological problem. In: Tikhomirov V, editor. Selected works of A.N. Kolmogorov. Springer; 1991. p. 242–70.
- [12] Ngamsaad W, Khompurngson K. Self-similar solutions to a density-dependent reaction-diffusion model. *Phys Rev E* 2012;85:066120.
- [13] Cho H, Jónsson H, Campbell K, Melke P, Williams JW, Jedynak B. Self-organization in high-density bacterial colonies: Efficient crowd control. *PLoS Biol* 2007;5(11):e302. doi:10.1371/journal.pbio.0050302.
- [14] Volfson D, Cookson S, Hasty J, Tsimring LS. Biomechanical ordering of dense cell populations. *Proc Natl Acad Sci USA* 2008;105(40):15346–51.
- [15] Mather W, Mondragón-Palomino O, Danino T, Hasty J, Tsimring L. Streaming instability in growing cell populations. *Phys Rev Lett* 2010;104:208101. doi:10.1103/PhysRevLett.104.208101.
- [16] Boyer D, Mather W, Mondragón-Palomino O, Orozco-Fuentes S, Danino T, Hasty J, et al. Buckling instability in ordered bacterial colonies. *Phys Biol* 2011;8(2):026008. <http://stacks.iop.org/1478-3975/8/i-2/a=026008>
- [17] Su PT, Liao CT, Roan JR, Wang SH, Chiou A, Syu WJ. Bacterial colony from two-dimensional division to three-dimensional development. *PLoS ONE* 2012;7(11):e48098. doi:10.1371/journal.pone.0048098.
- [18] Grant MAA, Waclaw B, Allen RJ, Cicuta P. The role of mechanical forces in the planar-to-bulk transition in growing *Escherichia coli* microcolonies. *J R Soc Interface* 2014;11(97):20140400.
- [19] Farrell F, Hallatschek O, Marenduzzo D, Waclaw B. Mechanically driven growth of quasi-two-dimensional microbial colonies. *Phys Rev Lett* 2013;111(16):168101.
- [20] Cates ME. Diffusive transport without detailed balance in motile bacteria: does microbiology need statistical physics? *Rep Prog Phys* 2012;75(4):042601. <http://stacks.iop.org/0034-4885/75/i=4/a=042601>
- [21] Bruna M, Chapman SJ. Diffusion of multiple species with excluded-volume effects. *J Chem Phys* 2012a;137(20):204116. doi:10.1063/1.4767058.
- [22] Bodnar M, Velazquez JJL. Derivation of macroscopic equations for individual cell-based models: a formal approach. *Math Methods Appl Sci* 2005;28(15):1757–79. doi:10.1002/mma.638.
- [23] Lushnikov PM, Chen N, Alber M. Macroscopic dynamics of biological cells interacting via chemotaxis and direct contact. *Phys Rev E* 2008;78:061904. doi:10.1103/PhysRevE.78.061904.
- [24] Simpson MJ, Baker RE, McCue SW. Models of collective cell spreading with variable cell aspect ratio: A motivation for degenerate diffusion models. *Phys Rev E* 2011;83:021901. doi:10.1103/PhysRevE.83.021901.
- [25] Baker RE, Simpson MJ. Models of collective cell motion for cell populations with different aspect ratio: Diffusion, proliferation and travelling waves. *Physica A* 2012;391(14):3729–50. doi:10.1016/j.physa.2012.01.009.
- [26] Bruna M, Chapman SJ. Excluded-volume effects in the diffusion of hard spheres. *Phys Rev E* 2012b;85:011103. doi:10.1103/PhysRevE.85.011103.
- [27] Dyson L, Maini PK, Baker RE. Macroscopic limits of individual-based models for motile cell populations with volume exclusion. *Phys Rev E* 2012;86:031903. doi:10.1103/PhysRevE.86.031903.
- [28] Penington CJ, Hughes BD, Landman KA. Interacting motile agents: Taking a mean-field approach beyond monomers and nearest-neighbor steps. *Phys Rev E* 2014;89:032714. doi:10.1103/PhysRevE.89.032714.
- [29] Almet AA, Pan M, Hughes BD, Landman KA. When push comes to shove: Exclusion processes with nonlocal consequences. *Physica A* 2015;437(0):119–29. doi:10.1016/j.physa.2015.05.031.
- [30] Eberl HJ, Demaret L. A finite difference scheme for a degenerated diffusion equation arising in microbial ecology. *Electron J Differ Equ* 2007;15:77–95.
- [31] Jalbert E, Eberl HJ. Numerical computation of sharp travelling waves of a degenerate diffusion reaction equation arising in biofilm modelling. *Commun Nonlinear Sci Numer Simul* 2014;19(7):2181–90. doi:10.1016/j.cnsns.2013.11.001.
- [32] Harko T, Mak MK. Travelling wave solutions of the reaction-diffusion mathematical model of glioblastoma growth: An Abel equation based approach. *Math Biosci Eng* 2015;12(1):41–69. doi:10.3934/mbe.2015.12.41. <http://aims sciences.org/journals/displayArticlesnew.jsp?paperID=10615>
- [33] Arciero JC, Mi Q, Branca MF, Hackam DJ, Swigon D. Continuum model of collective cell migration in wound healing and colony expansion. *Biophys J* 2011;100(3):535–43.
- [34] Tonks L. The complete equation of state of one, two and three-dimensional gases of hard elastic spheres. *Phys Rev* 1936;50:955–63. doi:10.1103/PhysRev.50.955.
- [35] Salsburg ZW, Zwanzig RW, Kirkwood JG. Molecular distribution functions in a one dimensional fluid. *J Chem Phys* 1953;21(6):1098–107. doi:10.1063/1.1699116.
- [36] Helfand E, Frisch HL, Lebowitz JL. Theory of the two and one dimensional rigid sphere fluids. *J Chem Phys* 1961;34(3):1037–42. doi:10.1063/1.1731629.

- [37] Takatori SC, Yan W, Brady JF. Swim pressure: Stress generation in active matter. *Phys Rev Lett* 2014;113:028103. doi:[10.1103/PhysRevLett.113.028103](https://doi.org/10.1103/PhysRevLett.113.028103).
- [38] Takatori SC, Brady JF. Towards a thermodynamics of active matter. *Phys Rev E* 2015;91:032117. doi:[10.1103/PhysRevE.91.032117](https://doi.org/10.1103/PhysRevE.91.032117).
- [39] Solon AP, Stenhammar J, Wittkowski R, Kardar M, Kafri Y, Cates ME, et al. Pressure and phase equilibria in interacting active Brownian spheres. *Phys Rev Lett* 2015;114:198301. doi:[10.1103/PhysRevLett.114.198301](https://doi.org/10.1103/PhysRevLett.114.198301).
- [40] Harvey CW, Alber M, Tsimring LS, Aranson IS. Continuum modeling of myxobacteria clustering. *New J Phys* 2013;15(3):035029. <http://stacks.iop.org/1367-2630/15/i=3/a=035029>
- [41] Garduño FS, Maini P. Traveling wave phenomena in some degenerate reaction-diffusion equations. *J Differ Equ* 1995;117(2):281–319. doi:[10.1006/jdeq.1995.1055](https://doi.org/10.1006/jdeq.1995.1055).
- [42] Garduño FS, Maini P. An approximation to a sharp type solution of a density-dependent reaction-diffusion equation. *Appl Math Lett* 1994;7(1):47–51. doi:[10.1016/0893-9659\(94\)90051-5](https://doi.org/10.1016/0893-9659(94)90051-5).
- [43] Arfken GB. *Mathematical methods for physicists*. San Diego: Academic Press; 1985.
- [44] Press WH, Flannery BP, Teukolsky SA, Vetterling WT. *Numerical recipes in C: The art of scientific computing*. Cambridge: Cambridge University Press; 1988.
- [45] Sokolov A, Aranson IS, Kessler JO, Goldstein RE. Concentration dependence of the collective dynamics of swimming bacteria. *Phys Rev Lett* 2007;98:158102. doi:[10.1103/PhysRevLett.98.158102](https://doi.org/10.1103/PhysRevLett.98.158102).
- [46] Rabani A, Ariel G, Be'er A. Collective motion of spherical bacteria. *PLoS ONE* 2013;8(12):e83760. doi:[10.1371/journal.pone.0083760](https://doi.org/10.1371/journal.pone.0083760).